

# Point Mutation of the Proteasome $\beta 5$ Subunit Gene Is an Important Mechanism of Bortezomib Resistance in Bortezomib-Selected Variants of Jurkat T Cell Lymphoblastic Lymphoma/Leukemia Line

Shuqing Lü, Jianmin Yang, Xianmin Song, Shenglan Gong, Hong Zhou, Lieping Guo, Ningxia Song, Xiaochen Bao, Pingping Chen, and Jianmin Wang

Department of Hematology, Changhai Hospital, Second Military Medical University, Shanghai, China

## ABSTRACT

To study the mechanism of acquired resistance to bortezomib, a new antitumor drug that is the first therapeutic proteasome inhibitor, we established a series of bortezomib-resistant T lymphoblastic lymphoma/leukemia cell lines, designated the JurkatBs, from the parental Jurkat line via repeated drug selection. There were no significant differences in the growth curves or colony formation between the JurkatB cells and parental Jurkat cells. The effects of bortezomib on cytotoxicity, cell cycle arrest, and induction of apoptosis were decreased in JurkatB cells compared with parental Jurkat cells. A mutation in the proteasome  $\beta 5$  subunit (PSMB5) gene (G322A), which encodes an amino acid

change from Ala to Thr at polypeptide position 108, was detected by sequencing full-length cDNA clones and direct polymerase chain reaction products of the PSMB5 gene. Bortezomib caused less inhibition of chymotrypsin-like activity in resistant cells. When the G322A mutant PSMB5 was retrovirally introduced into parental Jurkat cells, it conferred bortezomib resistance to these cells, resulting in decreased cytotoxicity, apoptosis, and inhibition of chymotrypsin-like activity. The predicted structure of A108T-mutated PSMB5 shows a conformational change that suggests decreased affinity to bortezomib. In short, the G322A mutation of the PSMB5 gene is a novel mechanism for bortezomib resistance.

The proteasome has been well recognized as a valid target for antitumor therapy (Daniel et al., 2005; Rajkumar et al., 2005). Due to its essential role in the degradation of cellular proteins, the ubiquitin-proteasome pathway is involved in a variety of cellular processes, including transcriptional regulation, cell cycle progression, proliferation, and apoptosis (Voges et al., 1999). Within the core 20S catalytic complex of a proteasome,  $\beta 5$ ,  $\beta 2$ ,  $\beta 1$ , subunits are, respectively, related to the chymotrypsin-like, trypsin-like, and peptidylglutamyl-like activities. The chymotrypsin-like activity of the proteasome  $\beta 5$  subunit (PSMB5) is critical for the rate-limiting step of proteolysis. It is conformationally flexible with active catalytic sites located on the inner surface of the cylinder where protein substrates bind (Rivett, 1989; Löwe et al., 1995; Chen and Hochstrasser, 1996).

Bortezomib (pyrazylcarbonyl-Phe-Leu-boronate; PS-341),

This work was supported by the Chinese Shanghai Science and Technology Committee, Shanghai Nature Fund 07ZR14146.

Article, publication date, and citation information can be found at <http://jpet.aspetjournals.org>.  
doi:10.1124/jpet.108.138131.

a proteasome inhibitor, contains a boronate moiety linked to a dipeptide and has exceedingly high affinity, specificity, and selectivity for the chymotrypsin-like activity of the proteasome (Lightcap et al., 2000; Hideshima et al., 2001). Clinical studies have demonstrated the safety and promising efficacy of bortezomib against multiple myeloma and several relapsed or refractory non-Hodgkin's lymphoma subtypes (Goy et al., 2005; Richardson et al., 2005; Leonard et al., 2006). Additional trials are ongoing to define the full utility of this drug in other tumor types, including leukemia (Orlowski et al., 2002; Zavrski et al., 2007). Bortezomib is highly cytotoxic to adult T-lymphocytic leukemia (ATL) cells in vitro and in vivo (Satou et al., 2004; Nasr et al., 2005). The in vitro evidence of antileukemic effect and transient hematological improvements observed in some patients suggest that further investigation of bortezomib in acute leukemias, probably in combination with other agents, is warranted (Cortes et al., 2004; Horton et al., 2006).

Resistance to bortezomib develops in the majority of clinical patients treated with this single agent (Cheriyath et al.,

**ABBREVIATIONS:** PSMB5, proteasome  $\beta 5$  subunit; HSP, heat shock protein; JurkatB, Jurkat cells resistant to bortezomib; PI, propidium iodide; PCR, polymerase chain reaction; AMC, 7-amido-4-methylcoumarin; LLVY-AMC, *N*-succinyl-Leu-Leu-Val-Tyr-7-amido-4-methylcoumarin; Jurkat-PSMB5 cells, Jurkat cells transduced with the G322A mutant PSMB5 gene; Jurkat-EGFP cells, Jurkat cells transduced with PLEGFPN1 vector; MDR, multiple drug resistance.

2007). It is unfortunate that the mechanisms of resistance to bortezomib are poorly understood. One possibility is the up-regulation of pathways that suppress apoptosis. It has been reported that overexpression of heat shock protein (HSP)27 is associated with bortezomib resistance in lymphoma cells (Chauhan et al., 2003). It was also found that interleukin-6 and insulin-like growth factor-1 in the microenvironment can confer resistance to bortezomib (Chauhan et al., 2004). Microarray analysis revealed that HSP27, HSP70, HSP90, and T-cell factor 4 were expressed at a higher level in a bortezomib-resistant SHDHL-4 cell line, which was isolated from a screen for the bortezomib response of various cell lines originating from B-cell malignancies (Shringarpure et al., 2006). Because bortezomib is a molecule that targets an enzyme and directly inhibits the enzyme activity, we propose that there may be a wider variety of mechanisms underlying bortezomib resistance. For example, many patients with chronic myeloid leukemia or gastrointestinal stromal tumors who underwent therapy with the Bcr-Abl tyrosine kinase inhibitor, imatinib, eventually relapsed due to the appearance of mutations and amplification of the Bcr-Abl gene (Gorre et al., 2001; Mahadevan et al., 2007; Mughal and Goldman, 2007). Point mutations have also been shown to result in resistance to the c-KIT kinase inhibitors (Roberts et al., 2007).

To investigate possible similar mechanisms of resistance to bortezomib, we established bortezomib-resistant lymphoblastic lymphoma/leukemia cell lines, designated the JurkatBs, by repeated cycles of drug exposure and selection. A point mutation was discovered within the PSMB5 gene, representing a new mechanism underlying bortezomib resistance.

## Materials and Methods

**Cell Culture and Bortezomib Selection.** The Jurkat cell line was kindly provided by Dr. J. H. Kang (Cell Institute of the Academy of Science, Shanghai, China). Cells in log-phase growth were treated with bortezomib (Millennium Pharmaceuticals, Cambridge, MA) for 72 h initially at 1 nM (nearly 72 h  $IC_{50}$ ), 5 nM (nearly 72 h  $IC_{75}$ ), 10 nM (nearly 72 h  $IC_{90}$ ), or 200 nM (>72 h  $IC_{99}$ ). Cells were then cultured in drug-free culture medium containing 20% fetal bovine serum and treated with bortezomib for an additional 72 h when cell growth recovered. If the recovery time for cell growth was longer than 2 weeks, the selection cycle was repeated at the same concentration. If cell growth recovered within 2 weeks, the drug concentration was increased to the next step. After repeated rounds of bortezomib selection over a period of 6 months, the established resistant cell lines were designated "JurkatB" lines. Subclones were established from these lines by limiting dilution. These JurkatB cells were cultured without bortezomib for 2 weeks before use for comparison studies.

**Cell Growth, Cytotoxicity, and Soft-Agar Colony Formation Assay.** JurkatB and parent Jurkat cells in logarithmic phase growth were seeded in 24-well plates at  $1 \times 10^4$ /ml in three replicates and cultured at 37°C with 5%  $CO_2$  in a humidified incubator. The live cells were counted by trypan blue dye exclusion assay daily for 7 days. For analysis of cytotoxicity, cells seeded in 24-well plates were treated with bortezomib at a series of concentrations for 24 or 48 h. Numbers of live cells were determined by counting using a trypan blue assay, and survival percentages were calculated. Meanwhile, logarithmically growing cells were plated at  $1 \times 10^3$ /ml in RPMI 1640 medium with 20% fetal bovine serum and 3% agar. Colonies (>75  $\mu$ m) were counted on the 10th day.

**Cell Cycle and Apoptosis Analysis.** Jurkat and JurkatB cells treated with bortezomib along with untreated controls were washed

with phosphate-buffered saline, then fixed in 70% ethanol overnight at  $-20^\circ C$ , treated with RNaseA (Sigma-Aldrich, St. Louis, MO), stained with propidium iodide (PI) (Sigma-Aldrich), and assayed for DNA content by flow cytometry (BD Biosciences, San Jose, CA). The acquired histograms were analyzed by ModFit LT software (Verity Software House, Topsham, ME) to determine the cell cycle phase distribution. For analysis of induction of apoptosis, cells treated with bortezomib along with untreated control cells were stained with Annexin V/PI (BD Pharmingen, San Diego, CA) according to the product instructions. Cells were then analyzed for apoptosis by flow cytometry using the CellQuest software (BD Biosciences).

**DNA Sequencing.** Total RNA was extracted from Jurkat and JurkatB cells using TRIzol reagent (Invitrogen, Carlsbad, CA) according to the manufacturer's instructions. cDNA was amplified by polymerase chain reaction (PCR) using high-fidelity Taq DNA polymerase (GenScript, Piscataway, NJ). The primers were as follows: forward, 5'-GAT ATG GCG CTT GCC AGC GTG TT-3'; reverse, 5'-GAT TCA GGG GGT AGA GCC ACT ATA CTT CT-3'. The PCR products were isolated by agarose gel electrophoresis, cloned into the pGEM-T cloning vector (Promega, Madison, WI), and transformed into DH5 $\alpha$  *Escherichia coli* (GenScript). Clones were selected for sequencing of whole-length cDNA (ABI3730; Applied Biosystems, Foster City, CA). Direct sequencing of the PCR products was also performed after a point mutation was found.

**Proteasome Chymotrypsin-Like Activity Assay.** Cells in log-phase growth ( $1 \times 10^7$ ) treated with bortezomib and untreated control cells were lysed in 20 mM Tris-HCl buffer, pH 7.6, by repeated freezing in liquid nitrogen and thawing in a 37°C water bath. The chymotrypsin-like activity in the cell lysate was assayed by measuring release of the fluorophore, 7-amido-4-methylcoumarin (AMC), from the substrate *N*-succinyl-Leu-Leu-Val-Tyr-7-amido-4-methylcoumarin (LLVY-AMC, 10  $\mu$ M; Sigma-Aldrich). Fluorescence was measured on a Flexstation microplate fluorometer (Molecular Devices, Sunnyvale, CA) at excitation/emission wavelengths of 380/440 nm (Lightcap et al., 2000).

**Retroviral Infection.** For construction of the mutant human PSMB5 retrovirus vector (PLEGFP-mPSMB5), the mutated PSMB5 cDNA obtained from the JurkatB cells was amplified by PCR, restricted with BamHI and HindIII (New England Biolabs, Ipswich, MA), identified by sequencing, then subcloned into the PLEGFPN1 vector, transformed into DH5 $\alpha$ , and clones were selected under ampicillin. The PT67 packaging cell line was transfected with the PLEGFP-mPSMB5 or PLEGFPN1 plasmids using Lipofectamine 2000 (Invitrogen) for 48 h. The Jurkat cell line was infected with the viral supernatants from PT67 cells for 48 h and then selected with 100  $\mu$ g/ml G-418. The following day, Jurkat cells transduced with PLEGFP-mPSMB5 (Jurkat-mPSMB5) or PLEGFPN1 (Jurkat-EGFP) were cultured for analysis of cytotoxicity, apoptosis, and assay of proteasome chymotrypsin-like activity as described above.

**Statistical Analysis.** Data represent the mean  $\pm$  S.D. The significance of differences observed between experimental results was determined by  $\chi^2$  test and one-way ANOVA using the SPSS 11.5 software program (SPSS Inc., Chicago, IL).  $P < 0.05$  was considered to be significant.

## Results

**Establishment of T Lymphoblastic Lymphoma/Leukemia Cell Lines Resistant to the Proteasome Inhibitor Bortezomib.** A series of bortezomib-resistant T lymphoblastic lymphoma/leukemia cell lines, designated JurkatB1–JurkatB5, was established from the parental Jurkat line by repeated cycles of drug selection. One of these lines, which was named JurkatB2, was selected initially at 1 nM bortezomib. The concentration was increased by 2 to 5-fold each step according to the recovery time for cell growth. After reaching 200 nM, the selection concentration was increased

by 100 nM at each step until the concentration attained 500 nM. The JurkatB1, JurkatB3, and JurkatB4 lines were initially selected at 1, 5, and 10 nM, respectively; the increment of each step was 5 to 20 nM, then 100 nM after the concentration was greater than 200 nM. The JurkatB5 was initially selected at 200 nM repeatedly for 5 cycles, then increased by 100 nM at each step until reaching 500 nM. Some of the JurkatB lines were further selected with bortezomib for an additional 3 months, ending at 1000 nM and designated JurkatB/1000. Several subclones were obtained from the JurkatB lines by limiting dilution.

**There Are No Significant Differences in the Characteristics of Cellular Biology between Jurkat and JurkatB Cell Lines.** Jurkat and JurkatB cells in logarithmic phase growth were plated and counted daily for 7 days. The results revealed that the differences of cell counts between these lines were not significant at all time points. The doubling times of Jurkat, JurkatB2, and JurkatB2/1000 were 24.9, 25.4, and 24.6 h, respectively (Fig. 1A). There were also no significant differences in soft-agar colony formation efficiencies between these lines (Fig. 1B).

**Decreased Effect of Bortezomib in the Cytotoxicity, Cell Cycle Arrest, and Induction of Apoptosis on JurkatB Cells Compared with Parental Jurkat Cells.** To confirm the resistance of JurkatB cells to bortezomib (chem-

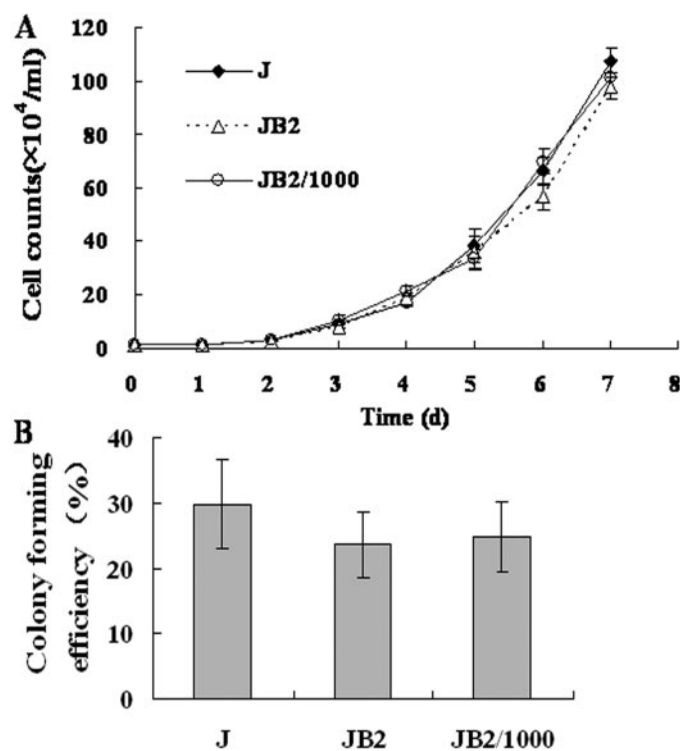


**Fig. 1.** Growth curves and colony-forming efficiencies of Jurkat and JurkatB cells. A, Jurkat (J), JurkatB2 (JB2), and JurkatB2/1000 (JB2/1000) cells in logarithmic phase growth were plated at  $1 \times 10^4$ /ml. Samples were taken daily to determine cell number. Live cells were counted using trypan blue dye exclusion. Data are shown as mean  $\pm$  S.D. of triplicate samples. The differences of cell counts were not significant between these lines at each day point ( $P > 0.05$ ). B, colonies ( $>75 \mu\text{m}$ ) of Jurkat and JurkatB cells were counted on the 10th day after plating in 3% agar. Data are displayed as mean  $\pm$  S.D. in sextuplet samples. The differences were not significant between Jurkat, JurkatB2, and JurkatB2/1000 lines ( $P > 0.05$ ).

ical structure shown in Fig. 2A) (Adams, 2004), the cytotoxic effects of bortezomib were first measured. The percentages of surviving JurkatB cells after treatment with a range of bortezomib concentrations for 24 (Fig. 2B) or 48 h (Fig. 2C) were significantly greater than those of Jurkat cells. The 24 and 48-h  $\text{IC}_{50}$  of bortezomib for Jurkat, JurkatB2, and JurkatB2/1000 lines were 10 and 3 nM, 26 and 12 nM, and 268 and 164 nM, respectively. To observe bortezomib-induced cell cycle arrest in these cells, Jurkat and JurkatB cells were assayed by flow cytometry after exposure to 50 nM bortezomib for 24 h along with untreated controls. The results showed no statistically significant difference between untreated JurkatB2, JurkatB2/1000, and Jurkat cells with respect to cell cycle distribution (representative experiment in Fig. 2D). Jurkat cells were arrested greatly at  $G_2$  phase after bortezomib treatment, but the effect of  $G_2$  arrest was decreased in JurkatB cells (Fig. 2D).  $G_2$  fractions in JurkatB2 and JurkatB2/1000 cells after bortezomib treatment were significantly lower than those of Jurkat cells ( $21.57 \pm 1.38$ ,  $14.09 \pm 2.17$ , and  $44.62 \pm 2.07\%$ , respectively) (Fig. 2E). The apoptotic effects of bortezomib were next investigated using Annexin V/PI staining by flow cytometry. This analysis revealed that at 24 and 48 h, the Annexin V/PI-positive cell ratios were significantly smaller in JurkatB cells compared with Jurkat cells, especially in JurkatB2/1000 cells (Fig. 2, F and G).

**G322A Point Mutation in the PSMB5 Gene Results in Decreased Inhibitory Effect of Bortezomib on the Chymotrypsin-Like Activity in JurkatB Lines.** To determine whether any mutations within the PSMB5 gene may have arisen in the bortezomib-resistant cells, the full-length cDNAs of PSMB5 were amplified by reverse transcription-PCR from Jurkat and JurkatB2 cells, then cloned into the PGEM-T Easy cloning vector, and transformed into *E. coli* (DH5 $\alpha$ ). Clones were randomly selected for sequencing. The nucleotide sequences from JurkatB cells were compared with the wild-type PSMB5 sequence from parental Jurkat cells and the existing GenBank overlap sequences (NP002788 and NP002797). No nucleotide differences were observed between the wild-type PSMB5 DNA sequences isolated from Jurkat cells and the existing GenBank database standard (Fig. 3A). Point mutations at nucleotide positions 192 (T to C) (data not shown) and 322 (G to A) were found in the JurkatB2 cells (Fig. 3B). The T192C mutation is silent, and the G322A point mutation results in an amino acid substitution (Ala108Thr). Independent reverse transcription-PCR products from JurkatB2 cells were also sequenced directly. The same alteration was found at position 192 (T to C) and was homogeneous. The nucleotide at 322 was heterogeneous (a doublet peak of A and G) (Fig. 3C), resulting in two possible products alternately containing an Ala or Thr. The JurkatB2 cells were further selected with bortezomib at concentrations as high as 700 to 1000 nM, and some clones were selected by limiting dilutions. Direct sequencing of the PSMB5 PCR products was then performed. This time, the results revealed only an A at position 322 (Fig. 3, D and E). The G322A mutation was further confirmed by sequencing the PSMB5 gene in other JurkatB lines (the same change from a doublet peak of A and G at position 322 in JurkatB1, JurkatB3, and JurkatB5 to exclusive A in sublines recovered from 700-1000 nM bortezomib).

Jurkat and JurkatB2 cells were incubated with 10 nM bortezomib for 6, 18, 24, or 48 h and then assessed for

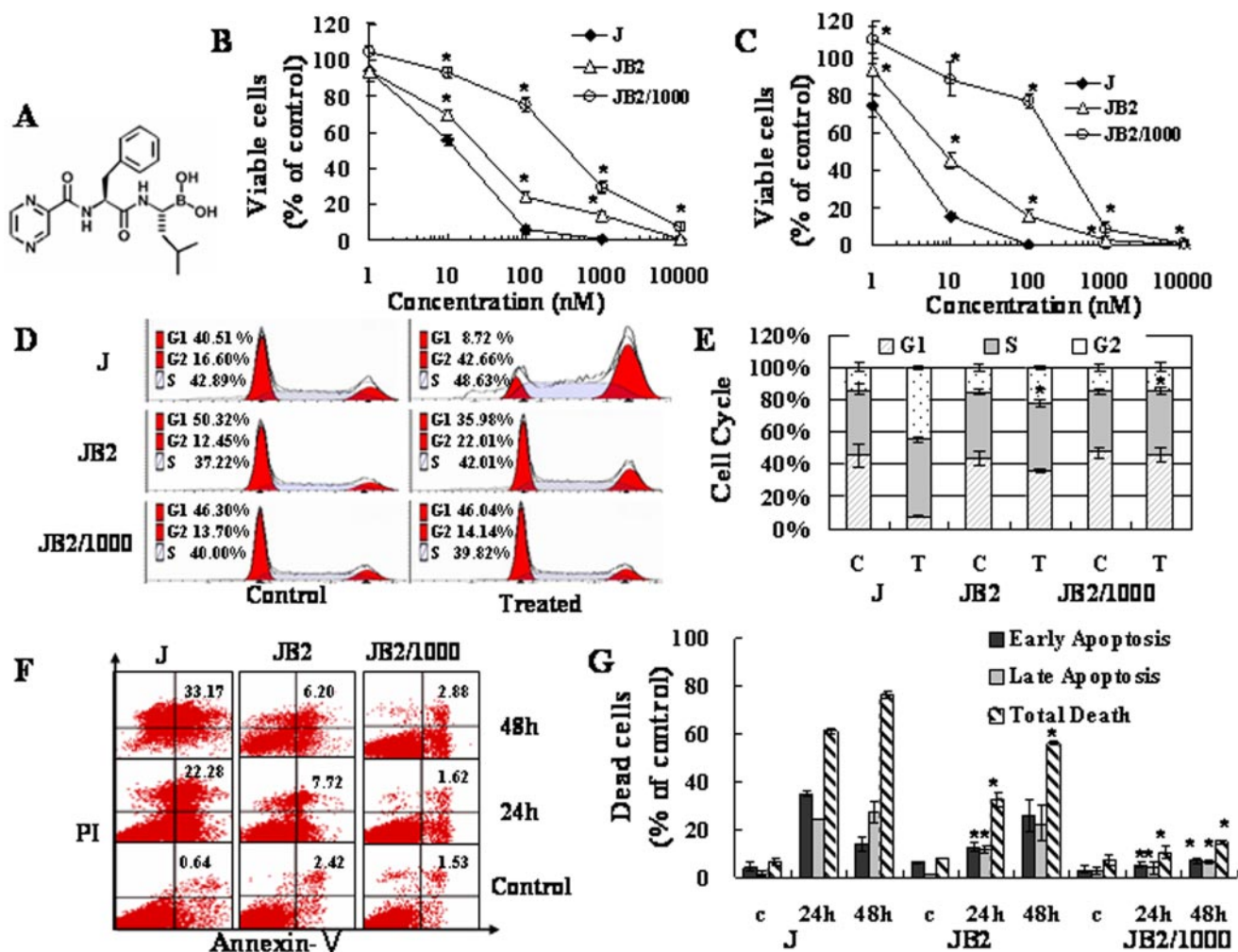


**Fig. 2.** Decreased cytotoxicity, cell cycle arrest, and induction of apoptosis by bortezomib on JurkatB cells compared with parental Jurkat cells. A, chemical structure of bortezomib. B and C, percentages of viable cells after treatment with a range of bortezomib concentrations for 24 (B) or 48 h (C). D, untreated control cells (left panels) and cells treated with 50 nM bortezomib for 24 h (middle) or 48 h (top) were analyzed for DNA content by flow cytometry. E, graphical representation of the data displayed in D as mean  $\pm$  S.D. of three independent experiments. F, untreated control cells (bottom) and cells treated with 50 nM bortezomib for 24 (middle) or 48 h (top) were stained with Annexin V/PI and analyzed by flow cytometry. Annexin V single-positive cells were considered early apoptotic; PI single-positive cells necrotic; and Annexin V and PI double-positive cells were considered late apoptotic (labeled with the percentage of gated cells). G, graphical representation of the data displayed in F as mean  $\pm$  S.D. of three independent experiments. \*,  $P < 0.05$  compared with Jurkat cells, in B, C, E, and G.

chymotrypsin-like activity against LLVY-AMC. The percentage inhibition of chymotrypsin-like activity was calculated according to the following equation:  $\%I = 100 \times (1 - SpAI/SpAU)$ , where  $SpAI$  is the chymotrypsin-like activity in the presence of bortezomib and  $SpAU$  is the chymotrypsin-like activity in the absence of bortezomib (Lightcap et al., 2000). The inhibition of chymotrypsin-like activity in JurkatB2 cells was significantly decreased compared with Jurkat cells (Fig. 4A). To further confirm the relationship between the decreased inhibition by bortezomib on chymotrypsin-like activity and the newly identified PSMB5 mutation (G322A) in JurkatB cells, particularly the JurkatB2/1000 cells, which are homogeneous and homozygous for the A at site 322, JurkatB2/1000 cells were incubated with bortezomib for various times (Fig. 4B) and concentrations (Fig. 4C). After treatment, cell lysates were assayed for chymotrypsin-like activity. No significant inhibition of the chymotrypsin-like activity was observed in JurkatB2/1000 cells treated with 5 to 40 nM bortezomib, and only a slight inhibitory effect (relative activ-

ity to untreated control was  $90.8 \pm 2.5\%$ ) was observed after treatment with 80 nM bortezomib.

**Decreased Cytotoxicity, Induction of Apoptosis, and Inhibition of Chymotrypsin-Like Activity by Bortezomib on Retrovirally Transduced Jurkat-mPSMB5 Cells Compared with Jurkat Cells.** To confirm the relationship between bortezomib resistance and the Ala108Thr PSMB5 mutant, we engineered the G322A-mutated PSMB5 gene into Jurkat cells using the retroviral vector (PLEGFP-mPSMB5). Jurkat cells transduced with the PLEGFP-mPSMB5). Jurkat cells transduced with the PLEGFPN1 vector only (Jurkat-EGFP) were also produced as a control (Fig. 5A). Sequencing of the PCR products for the PSMB5 gene in Jurkat-mPSMB5 and Jurkat-EGFP cells were performed. As expected, this showed a doublet peak (G/A) at the 322 site in Jurkat-mPSMB5 cells and a single G at the 322 site in Jurkat-EGFP cells, indicating that wild-type and mutated PSMB5 genes were expressed simultaneously in retrovirally transduced Jurkat-mPSMB5 cells (Fig. 5B).

The cytotoxicities of bortezomib on Jurkat-mPSMB5 cells,

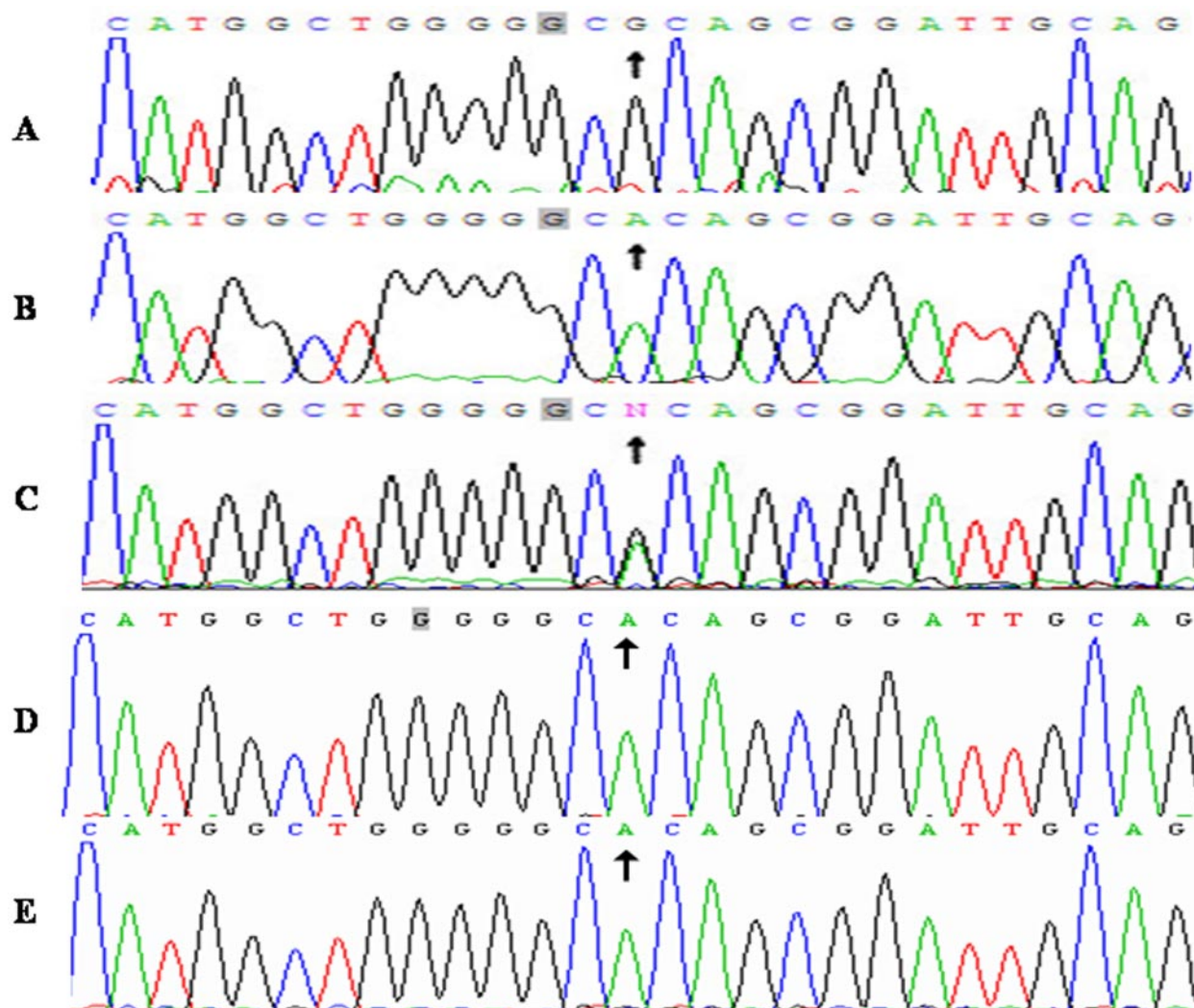


**Fig. 3.** G322A point mutation of PSMB5 gene in JurkatB cells. Sequences obtained by clone sequencing (position 322 marked with an arrow): A, parental Jurkat cells (322G); B, JurkatB2 cells (322A). Sequences obtained by direct PCR product sequencing: C, JurkatB2 cells (the doublet peak N at 322 is due to a mixture of G and A signals); D, a subclone of JurkatB2 cells (322A); E, JurkatB2/1000 cells (322A).

Jurkat-EGFP cells, and parental Jurkat cells were then investigated. The results showed that percentages of viable cells were significantly higher in Jurkat-mPSMB5 cells after treatment with bortezomib for 24 h at 1 to 50 nM than those in parental Jurkat cells, and the differences between Jurkat-EGFP and Jurkat cells were not significant (Fig. 5C). The apoptotic effects of bortezomib on Jurkat-mPSMB5 cells, Jurkat-EGFP cells, and Jurkat cells were investigated using Annexin V/PI staining by flow cytometry. Both early and late apoptosis after treatment with 50 nM bortezomib for 24 h were significantly less in Jurkat-mPSMB5 cells compared with Jurkat cells. As anticipated, there was no significant difference between Jurkat-EGFP cells and Jurkat cells (Fig. 5D).

Cell lines were assayed for chymotrypsin-like activity after treatment with bortezomib for various times (Fig. 5E) and at various concentrations (Fig. 5F). The inhibition of chymotrypsin-like activity in Jurkat-mPSMB5 cells was significantly decreased compared with parental Jurkat cells. There was also no significant difference between Jurkat-EGFP cells and Jurkat cells.

### Computer Modeling of the Mutant Structure Predicts a Conformational Change in the A108T Mutant PSMB5.

Based on the inhibition results, we would expect that the Thr substitution for Ala108 in the PSMB5 from bortezomib-resistant JurkatB cells contributes to a conformational change that results in a decreased binding affinity for the inhibitor to the chymotrypsin-like active site. To confirm this hypothesis, we modeled the structures of wild-type human PSMB5 and the A108T mutant based on the crystal structure of bovine PSMB5 (Unno et al., 2002) using the Cn3D4.1 software (Fig. 6). The predicted structure of A108T-mutated PSMB5 shows a substantially different conformation, especially at the cavate part in which residue 108 is located. This altered conformation may reduce the contacts between the inhibitor and the chymotrypsin-like active site, reducing the affinity for bortezomib.

### Discussion

Drug resistance is a major challenge to the treatment of leukemia and other tumors. Bortezomib, a new selective pro-

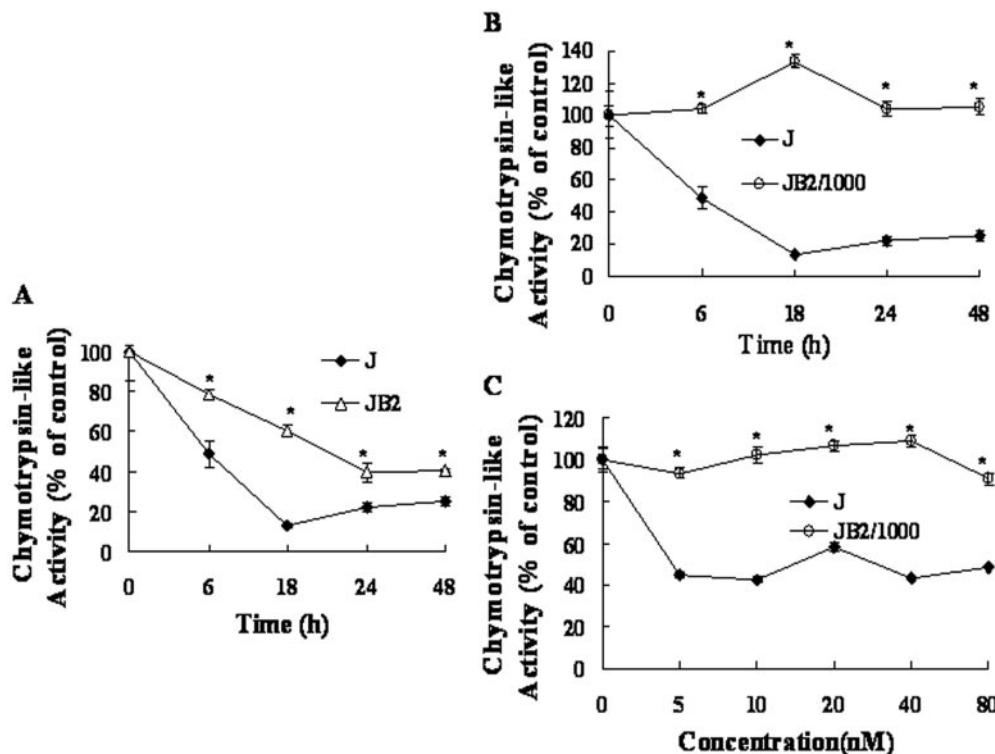


**Fig. 4.** Decreased inhibitory effect of bortezomib against chymotrypsin-like activity in JurkatB cells compared with Jurkat cells. A, Jurkat and JurkatB2 cells were incubated with 10 nM bortezomib for 6, 18, 24, or 48 h and assessed for chymotrypsin-like activity against LLVY-AMC; B and C, chymotrypsin-like activities in JurkatB2/1000 cells treated with 10 nM bortezomib for different times (B) or 5 to 80 nM bortezomib for 24 h (C) (\*,  $P < 0.05$  compared with Jurkat cells).

teasome inhibitor drug, not only promotes apoptosis in cancer cells, but it also sensitizes these cells to chemotherapy (Mitsiades et al., 2003; Dasmahapatra et al., 2006; Fribley et al., 2006). However, there are some patients who do not respond to bortezomib treatment, or who respond briefly but then relapse. To discover the potential mechanisms of acquired bortezomib resistance, JurkatB lines were established from the parental T lymphoblastic lymphoma/leukemia Jurkat line by a repeated series of drug selection cycles. Cytotoxicity, cell cycle arrest, and apoptosis induced by bortezomib were significantly decreased in the JurkatB cells compared with parental Jurkat cells, confirming that the JurkatB lines were bortezomib-resistant.

No significant differences in growth curves or colony formation efficiencies were found between JurkatB cells and parental Jurkat cells. Acquisition of bortezomib resistance did not alter the growth and colony-forming ability of JurkatB cells in the absence of drug.

No signs of drug efflux, cross-resistance to other chemotherapeutic drugs (daunorubicin, doxorubicin, vindesine, and etoposide), overexpression of MDR (multidrug resistance) gene 1 mRNA, or expression of P-glycoprotein were detected in JurkatB lines (data not shown). Thus, it is unlikely that a MDR effect is responsible for the bortezomib resistance of JurkatB cells, as has been the case in some other reports (Frankel et al., 2000; Shringarpure et al., 2006; Minderman et al., 2007).

A point mutation of the PSMB5 gene (G322A) was detected in JurkatB2 cells by clone sequencing. This nucleotide change causes an A108T substitution at the amino acid level. Direct sequencing results of PCR products of the PSMB5 gene from JurkatB2 cells indicated heterogeneity at the 322 site (G/A). Other than simple heterozygosity, perhaps with amplification of the mutant gene, another possible explanation is that there were two populations of cells in the

JurkatB2 line, one wild-type at position 322 and the other mutated. To investigate these possibilities, JurkatB2 cell line was further selected with a higher concentration of bortezomib (progressive to 1000 nM, labeled JurkatB2/1000 cells), and several subclones were established by limiting dilution. Direct sequencing of the PSMB5 gene PCR products from JurkatB2/1000 cells and these subclones were performed, revealing exclusive A at 322 position, indicating that the original result was due to polyclonality of the original line.

It is possible that a small population of random G322A mutant cells exist in the Jurkat line, but this population was too low to be detected using the sequencing procedure. The selection process, using gradually increasing concentrations of bortezomib, seemed to support the outgrowth of the mutant population, accompanied by survivors that do not have the mutation. The mutated cells have an apparent growth advantage over the wild-type in the presence of bortezomib; thus, the percentage of this population became increasingly larger under selection conditions, reaching the 322A monoclonality of the JurkatB2/1000 line. The outgrowth of G322A mutant cells was further confirmed by the sequencing results of PSMB5 gene in other JurkatB lines (the same change from G/A to A at 322 position), which were also selected from the Jurkat line by different initial concentrations and incremental concentration steps.

To identify the relationship between bortezomib resistance and the PSMB5 A108T mutant, the chymotrypsin-like activities of JurkatB and Jurkat cells were measured after bortezomib treatment. The inhibition of chymotrypsin-like activity in JurkatB cells was significantly decreased compared with parental Jurkat cells. Because the MDR mechanism had already been ruled out, it is unlikely that drug elimination by efflux pumps could account for the decreased inhibition of chymotrypsin-like activity in JurkatB cells. The chy-

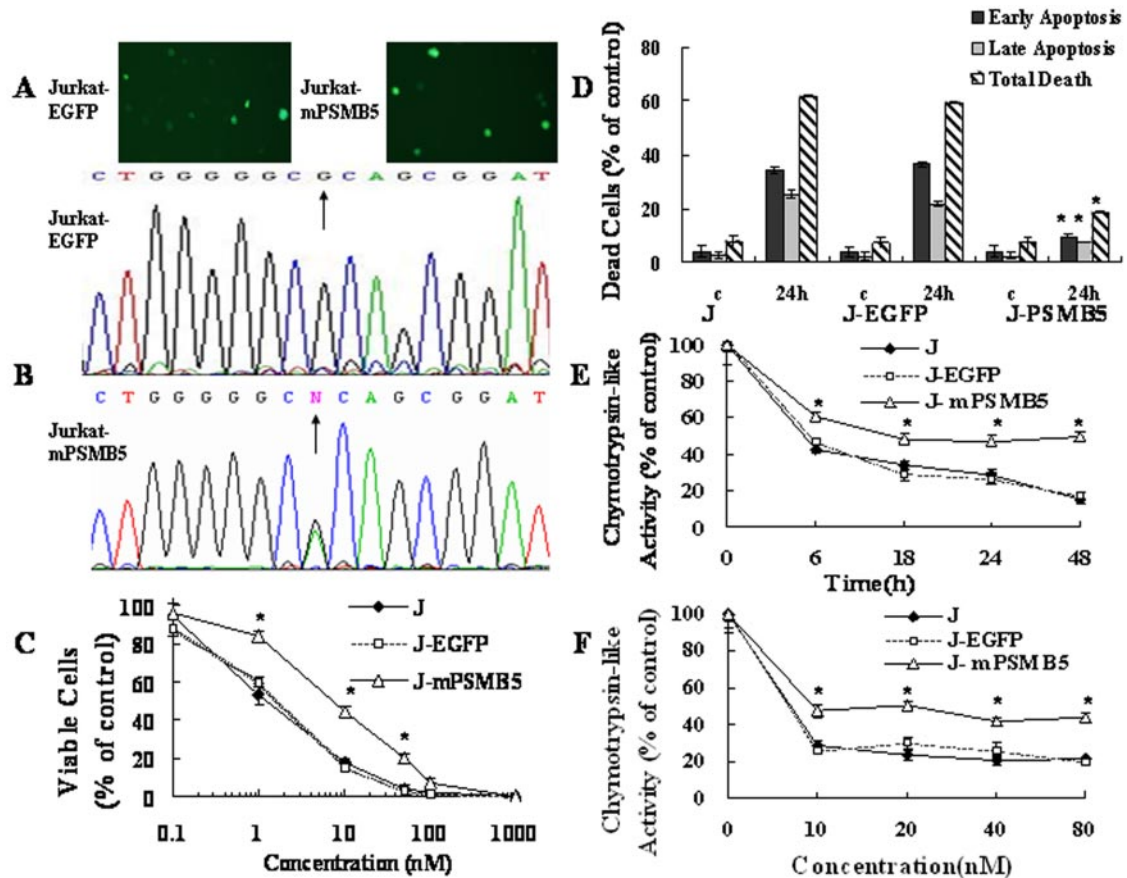


**Fig. 5.** Decreased cytotoxicity, induction of apoptosis, and inhibition of the chymotrypsin-like activity by bortezomib on retrovirally transduced Jurkat-mPSMB5 cells compared with Jurkat cells. A, green fluorescence expressed by Jurkat-mPSMB5 cells (right panel, Jurkat cells transduced with the G322A-mutant PSMB5 gene) and Jurkat-EGFP cells (left panel, Jurkat cells transduced with PLEGFPN1 vector only). B, sequencing of the PCR products of PSMB5 gene shows a single G in Jurkat-EGFP cells (top) and a doublet peak (G/A) at the 322 site in the Jurkat-mPSMB5 cells (bottom), indicating the wild-type and mutant PSMB5 genes both expressed in Jurkat-mPSMB5 cells. C, percentages of viable cells in Jurkat-mPSMB5 (J-mPSMB5) cells and Jurkat-EGFP (J-EGFP) cells after treatment with bortezomib of gradient concentrations for 24 h. D, early, late apoptosis and total death (Annexin V/PI) after treatment with 50 nM bortezomib for 24 h. Data are displayed as mean  $\pm$  S.D. of three independent experiments. E and F, cells were treated with 10 nM bortezomib for different times (E) or 10 to 80 nM bortezomib for 24 h (F) and assessed for chymotrypsin-like activity. \*,  $P < 0.05$  compared with Jurkat cells, in C, D, E, and F.

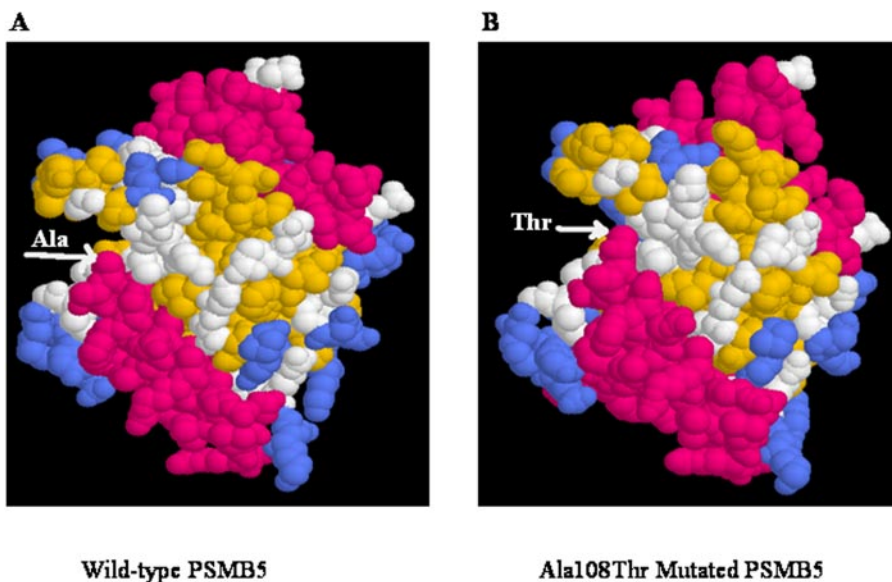


**Fig. 6.** Structural models of wild-type PSMB5 and mutant PSMB5. A, the model of wild-type PSMB5. The residue labeled with a white arrow is the Ala at position 108. B, the predicted structure of A108T-mutated PSMB5. The residue labeled with a white arrow is the Thr at position 108.

motrypsin-like activities in JurkatB2/1000 cells, which are uniform for the 322A base substitution, treated with different concentrations of bortezomib or for different times were

compared with untreated control cells, and the results showed a nearly complete loss of bortezomib-induced inhibition of chymotrypsin-like activity. Thus, we propose that the

A108T substitution of PSMB5 contributes to bortezomib resistance.

To further confirm this, the G322A mutant PSMB5 was retrovirally introduced into parental Jurkat cells. The retrovirally transduced Jurkat-mPSMB5 cells acquired a bortezomib-resistant phenotype due to the expression of G322A mutant PSMB5, reiterating the idea that the PSMB5 A108T mutation is an important mechanism of bortezomib resistance in JurkatB lines.

To date, biochemical and crystallographic characterization of the proteasome active site mutants has been performed only in yeast. Mutagenic inactivation of active site residues in the proteasome has revealed some striking phenotypes in that system. In particular, the T1A mutation within the active site of PSMB5 is lethal, and the K33A mutation causes severe growth defects (Seemüller et al., 1995).

The crystal structure of bortezomib bound to the yeast 20S proteasome illustrates that bortezomib adopts an antiparallel  $\beta$ -sheet conformation (Groll et al., 2002, 2006). These  $\beta$ -sheets are stabilized by direct hydrogen bonds between conserved residues of the proteasome  $\beta$  subunits and main chain atoms of the drug. The  $\beta 6$  Asp114O,  $\beta 5$  Ala49N, and  $\beta 5$  Ala50N coordinate tightly with the carbonyl oxygen of bortezomib. Bortezomib exhibits different binding affinities to distinct active sites due to interactions of the individual side chains of this inhibitor with certain cavate parts of the protein.

Our computer modeling of the A108T PSMB5 mutant suggests that a conformational change is incurred that may disrupt contacts between the chymotrypsin-like active site and bortezomib, resulting in the observed changes in inhibitory and proapoptotic activity.

Other than the same G322A mutation, overexpression of the PSMB5 mRNA was detected in highly resistant JurkatB5 and JurkatB1 cells that also originated from the parental Jurkat line (data not shown). Although bortezomib is a highly selective inhibitor to the chymotrypsin-like activity at PSMB5, other subunits such as PSMB6 may also contribute to interactions between this inhibitor and the active catalytic site, as has been described in yeast (Groll et al., 2006). Thus, mutations of these subunits should not be overlooked in the JurkatB lines. We also expect that other novel PSMB5 mutants may be selected with bortezomib at higher concentrations. Thus, further studies into more potential mechanisms of bortezomib resistance are necessary.

In summary, T lymphoblastic lymphoma/leukemia cell lines resistant to the proteasome inhibitor, bortezomib, can be established by repeated drug selection. The G322A point mutation of the PSMB5 gene is an important mechanism of bortezomib resistance in these JurkatB lines. The resistance to bortezomib seems to occur through a conformational change that reduces affinity between bortezomib and the chymotrypsin-like active site at PSMB5. The mechanism of bortezomib resistance conferred by PSMB5 mutant may also possibly occur in patient tumors, particularly those treated with single, low-dose bortezomib. Thus, it may be important to determine the sequence of the PSMB5 gene in tumors of patients who will be treated with bortezomib or in tumors that relapse from bortezomib therapy.

## References

Adams J (2004) The development of proteasome inhibitors as anticancer drugs. *Cancer Cell* **5**:417–421.

- Chauhan D, Li G, Shringarpure R, Podar K, Ohtake Y, Hideshima T, and Anderson KC (2003) Blockade of Hsp27 overcomes Bortezomib/proteasome inhibitor PS-341 resistance in lymphoma cells. *Cancer Res* **63**:6174–6177.
- Chauhan D, Li G, Podar K, Hideshima T, Mitsiades C, Schlossman R, Munshi N, Richardson P, Cotter FE, and Anderson KC (2004) Targeting mitochondria to overcome conventional and bortezomib/proteasome inhibitor PS-341 resistance in multiple myeloma (MM) cells. *Blood* **104**:2458–2466.
- Chen P and Hochstrasser M (1996) Autocatalytic subunit processing couples active site formation in the 20S proteasome to completion of assembly. *Cell* **86**:961–972.
- Cheriyath V, Jacobs BS, and Hussein MA (2007) Proteasome inhibitors in the clinical setting: benefits and strategies to overcome multiple myeloma resistance to proteasome inhibitors. *Drugs R D* **8**:1–12.
- Cortes J, Thomas D, Koller C, Giles F, Estey E, Faderl S, Garcia-Manero G, McConkey D, Ruiz SL, Guercioli R, et al. (2004) Phase I study of bortezomib in refractory or relapsed acute leukemias. *Clin Cancer Res* **10**:3371–3376.
- Daniel KG, Kuhn DJ, Kazi A, and Dou QP (2005) Anti-angiogenic and anti-tumor properties of proteasome inhibitors. *Curr Cancer Drug Targets* **5**:529–541.
- Dasmahapatra G, Nguyen TK, Dent P, and Grant S (2006) Adaphostin and bortezomib induce oxidative injury and apoptosis in imatinib mesylate-resistant hematopoietic cells expressing mutant forms of Bcr/Abl. *Leuk Res* **30**:1263–1272.
- Frankel A, Man S, Elliott P, Adams J, and Kerbel RS (2000) Lack of multicellular drug resistance observed in human ovarian and prostate carcinoma treated with the proteasome inhibitor PS-341. *Clin Cancer Res* **6**:3719–3728.
- Fribley AM, Evenchik B, Zeng Q, Park BK, Guan JY, Zhang H, Hale TJ, Soengas MS, Kaufman RJ, and Wang CY (2006) Proteasome inhibitor PS-341 induces apoptosis in cisplatin-resistant squamous cell carcinoma cells by induction of Noxa. *J Biol Chem* **281**:31440–31447.
- Gorre ME, Mohammed M, Ellwood K, Hsu N, Paquette R, Rao PN, and Sawyers CL (2001) Clinical resistance to STI-571 cancer therapy caused by BCR-ABL gene mutation or amplification. *Science* **293**:876–880.
- Goy A, Younes A, McLaughlin P, Pro B, Romaguera JE, Hagemeister F, Fayad L, Dang NH, Samaniego F, Wang M, et al. (2005) Phase II study of proteasome inhibitor bortezomib in relapsed or refractory B-cell non-Hodgkin's lymphoma. *J Clin Oncol* **23**:667–675.
- Groll M, Nazif T, Huber R, and Bogoy M (2002) Probing structural determinants distal to the site of hydrolysis that control substrate specificity of the 20S proteasome. *Chem Biol* **9**:655–662.
- Groll M, Berkers CR, Ploegh HL, and Ovaas H (2006) Crystal structure of the boronic acid-based proteasome inhibitor bortezomib in complex with the yeast 20S proteasome. *Structure* **14**:451–456.
- Hideshima T, Richardson P, Chauhan D, Palombella VJ, Elliott PJ, Adams J, Adams J, and Anderson KC (2001) The proteasome inhibitor PS-341 inhibits growth, induces apoptosis, and overcomes drug resistance in human multiple myeloma cells. *Cancer Res* **61**:3071–3076.
- Horton TM, Gannavarapu A, Blaney SM, D'Argenio DZ, Plon SE, and Berg SL (2006) Bortezomib interactions with chemotherapy agents in acute leukemia in vitro. *Cancer Chemother Pharmacol* **58**:13–23.
- Leonard JP, Furman RR, and Coleman M (2006) Proteasome inhibition with bortezomib: a new therapeutic strategy for non-Hodgkin's lymphoma. *Int Cancer* **119**:971–979.
- Lightcap ES, McCormack TA, Pien CS, Chau V, Adams J, and Elliott PJ (2000) Proteasome inhibition measurements: clinical application. *Clin Chem* **46**:673–683.
- Löwe J, Stock D, Jap B, Zwickl P, Baumeister W, and Huber R (1995) Crystal structure of the 20S proteasome from the archaeon *T. acidophilum* at 3.4 Å resolution. *Science* **268**:533–539.
- Mahadevan D, Cooke L, Riley C, Swart R, Simons B, Della Croce K, Wisner L, Iorio M, Shakalya K, Garewal H, et al. (2007) A novel tyrosine kinase switch is a mechanism of imatinib resistance in gastrointestinal stromal tumors. *Oncogene* **26**:3909–3919.
- Minderman H, Zhou Y, O'Loughlin KL, and Baer MR (2007) Bortezomib activity and in vitro interactions with anthracyclines and cytarabine in acute myeloid leukemia cells are independent of multidrug resistance mechanisms and p53 status. *Cancer Chemother Pharmacol* **60**:245–255.
- Mitsiades N, Mitsiades CS, Richardson PG, Poulaki V, Tai YT, Chauhan D, Fournarakis G, Gu X, Bailey C, Joseph M, et al. (2003) The proteasome inhibitor PS-341 potentiates sensitivity of multiple myeloma cells to conventional chemotherapeutic agents: therapeutic applications. *Blood* **101**:2377–2380.
- Mughal TI and Goldman JM (2007) Emerging strategies for the treatment of mutant Bcr-Abl T315I myeloid leukemia. *Clin Lymphoma Myeloma* **7** (Suppl 2):S81–S84.
- Nasr R, El-Sabban ME, Karam JA, Dbaibo G, Kfoury Y, Arnulf B, Lepelletier Y, Bex F, de Thé H, Hermine O, et al. (2005) Efficacy and mechanism of action of the proteasome inhibitor PS-341 in T-cell lymphomas and HTLV-I associated adult T-cell leukemia/lymphoma. *Oncogene* **24**:419–430.
- Orlowski RZ, Stinchcombe TE, Mitchell BS, Shea TC, Baldwin AS, Stahl S, Adams J, Esseltine DL, Elliott PJ, Pien CS, et al. (2002) Phase I trial of the proteasome inhibitor PS-341 in patients with refractory hematologic malignancies. *J Clin Oncol* **20**:4420–4427.
- Rajkumar SV, Richardson PG, Hideshima T, and Anderson KC (2005) Proteasome inhibition as a novel therapeutic target in human cancer. *J Clin Oncol* **23**:630–639.
- Richardson PG, Sonneveld P, Schuster MW, Irwin D, Stadtmauer EA, Facon T, Harousseau JL, Ben-Yehuda D, Lonial S, Goldschmidt H, et al. (2005) Assessment of proteasome inhibition for extending remissions (APEX) investigators. Bortezomib or high-dose dexamethasone for relapsed multiple myeloma. *N Engl J Med* **352**:2487–2498.
- Rivett AJ (1989) The multicatalytic proteinase. Multiple proteolytic activities. *J Biol Chem* **264**:12215–12219.
- Roberts KG, Odell AF, Byrnes EM, Baleato RM, Griffith R, Lyons AB, and Ashman LK (2007) Resistance to c-KIT kinase inhibitors conferred by V654A mutation. *Mol Cancer Ther* **6**:1159–1166.

- Satou Y, Nosaka K, Koya Y, Yasunaga JI, Toyokuni S, and Matsuoka M (2004) Proteasome inhibitor, bortezomib, potently inhibits the growth of adult T-cell leukemia cells both in vivo and in vitro. *Leukemia* **18**:1357–1363.
- Seemüller E, Lupas A, Stock D, Löwe J, Huber R, and Baumeister W (1995) Proteasome from *thermoplasma acidophilum*: a threonine protease. *Science* **268**:579–582.
- Shringarpure R, Catley L, Bhole D, Burger R, Podar K, Tai YT, Kessler B, Galardy P, Ploegh H, Tassone P, et al. (2006) Gene expression analysis of B-lymphoma cells resistant and sensitive to bortezomib. *Br J Haematol* **134**:145–156.
- Unno M, Mizushima T, Morimoto Y, Tomisugi Y, Tanaka K, Yasuoka N, and Tsukihara T (2002) The structure of the mammalian 20S proteasome at 2.75 Å resolution. *Structure* **10**:609–618.
- Voges D, Zwickl P, and Baumeister W (1999) The 26S proteasome: a molecular machine designed for controlled proteolysis. *Annu Rev Biochem* **68**:1015–1068.
- Zavrski I, Kleeberg L, Kaiser M, Fleissner C, Heider U, Sterz J, Jakob C, and Sezer O (2007) Proteasome as an emerging therapeutic target in cancer. *Curr Pharm Des* **13**:471–485.

---

**Address correspondence to:** Dr. Jianmin Wang, Department of Hematology, Changhai Hospital, Second Military Medical University, 174 Changhai Road, Shanghai 200433, China. E-mail: jmwang@medmail.com.cn

---